

Further explorations of Skyrme-Hartree-Fock-Bogoliubov mass formulas. II: Role of the effective mass.

S. Goriely,¹ M. Samyn,¹ M. Bender,² and J. M. Pearson³

¹*Institut d'Astronomie et d'Astrophysique, Université Libre de Bruxelles - CP226, 1050 Brussels, Belgium*

²*Service de Physique Nucléaire Théorique et de Physique Mathématique,*

Université Libre de Bruxelles - CP229, 1050 Brussels, Belgium

³*Dépt. de Physique, Université de Montréal, Montréal (Québec), H3C 3J7 Canada*

We have constructed four new complete mass tables, referred to as HFB-4 to HFB-7, each one including all the 9200 nuclei lying between the two drip lines over the range of Z and $N \geq 8$ and $Z \leq 120$. HFB-4 and HFB-5 have the isoscalar effective mass M_s^* constrained to the value $0.92M$, with the former having a density-independent pairing, and the latter a density-dependent pairing. HFB-6 and HFB-7 are similar, except that M_s^* is constrained to $0.8M$. The rms errors of the mass-data fits are 0.680, 0.675, 0.686, and 0.676 MeV, respectively, almost as good as for the HFB-2 mass formula, for which M_s^* was unconstrained. However, as usual, the single-particle spectra depend significantly on M_s^* . This decoupling of the mass fits from the fits to the single-particle spectra has been achieved only by making the cutoff parameter of the δ -function pairing force a free parameter. An improved treatment of the center-of-mass correction was adopted, but although this makes a difference to individual nuclei it does not reduce the overall rms error of the fit. The extrapolations of all four new mass formulas out to the drip lines are essentially the same as for the original HFB-2 mass formula.

PACS numbers: 21.10.Dr, 21.30.-x, 21.60.Jz

I. INTRODUCTION

In the last few years it has become possible to construct complete mass tables by the Hartree-Fock (HF) method [1, 2, 3, 4], with the parameters of the underlying forces being fitted to essentially all of the available mass data. These HF calculations are based on conventional Skyrme forces of the form

$$\begin{aligned} v_{ij} = & t_0(1+x_0P_\sigma)\delta(\mathbf{r}_{ij}) \\ & +t_1(1+x_1P_\sigma)\frac{1}{2\hbar^2}\{p_{ij}^2\delta(\mathbf{r}_{ij})+h.c.\} \\ & +t_2(1+x_2P_\sigma)\frac{1}{\hbar^2}\mathbf{p}_{ij}\cdot\delta(\mathbf{r}_{ij})\mathbf{p}_{ij} \\ & +\frac{1}{6}t_3(1+x_3P_\sigma)\rho^\gamma\delta(\mathbf{r}_{ij}) \\ & +\frac{i}{\hbar^2}W_0(\boldsymbol{\sigma}_i+\boldsymbol{\sigma}_j)\cdot\mathbf{p}_{ij}\times\delta(\mathbf{r}_{ij})\mathbf{p}_{ij}, \end{aligned} \quad (1)$$

and a δ -function pairing force acting between like nucleons treated either in the full Bogoliubov framework (HFB) [2, 3, 4], or the BCS approximation thereto (HFBCS) [1],

$$v_{pair}(\mathbf{r}_{ij}) = V_{\pi q} \left[1 - \eta \left(\frac{\rho}{\rho_0} \right)^\alpha \right] \delta(\mathbf{r}_{ij}), \quad (2)$$

where $\rho \equiv \rho(\mathbf{r})$ is the local density, and ρ_0 is its equilibrium value in symmetric infinite nuclear matter (INM). Only in the most recent paper [4] was the possibility of a density-dependent pairing force admitted; in the first three [1, 2, 3] we had $\eta = 0$. However, in all four HF mass formulas the strength parameter $V_{\pi q}$ was allowed to be different for neutrons and protons, and also to be slightly

stronger for an odd number of nucleons ($V_{\pi q}^-$) than for an even number ($V_{\pi q}^+$), i.e., the pairing force between neutrons, for example, depends on whether N is even or odd. The two HFB mass formulas [3, 4] add to the energy corresponding to the above force (and to the kinetic energy and Coulomb energy including the exchange term in Slater approximation) a phenomenological Wigner term of the form

$$\begin{aligned} E_W = & V_W \exp \left\{ -\lambda \left(\frac{N-Z}{A} \right)^2 \right\} \\ & + V'_W |N-Z| \exp \left\{ - \left(\frac{A}{A_0} \right)^2 \right\}; \end{aligned} \quad (3)$$

a somewhat simpler Wigner term was used in the HFBCS mass formula [1] and the first HFB mass formula [2].

An important question concerns the cutoff to be applied to the δ -function pairing force: both BCS and Bogoliubov calculations diverge if the space of single-particle (s.p.) states over which such a pairing force is allowed to act is not truncated. However, making such a cutoff is not simply a computational device but is rather a vital part of the physics, pairing being essentially a finite-range phenomenon. To represent such an interaction by a δ -function force is thus legitimate only to the extent that all high-lying excitations are suppressed, although how exactly the truncation of the pairing space should be made will depend on the precise nature of the real, finite-range pairing force. It was precisely our ignorance on this latter point that allowed us in Ref. [3] to exploit the cutoff as a new degree of freedom: we found an optimal mass fit with the spectrum of s.p. states ε_i

confined to lie in the range

$$E_F - \varepsilon_\Lambda \leq \varepsilon_i \leq E_F + \varepsilon_\Lambda, \quad (4)$$

where E_F is the Fermi energy of the nucleus in question, and ε_Λ is a free parameter. We shall adopt the same parametrization in the present paper.

The two most recent of our mass formulas [3, 4] had their forces, labeled BSk2 and BSk3, respectively, fitted to the 2135 nuclei with $Z, N \geq 8$ whose masses have been measured and compiled in the 2001 Atomic Mass Evaluation (AME) of Audi and Wapstra [5]. The essential difference between these two forces is that the pairing is density-independent in the case of BSk2 [3], while having a density dependence of the form (2), with the parameters η and α taking the values given by Garrido *et al.* [6], in the case of BSk3 [4] (no other choice for η and α leads to a significant improvement). The rms errors of these fits are 0.674 MeV [3] and 0.656 MeV [4], respectively; the slight superiority of the latter is too insignificant to imply that the mass data require the pairing to be density-dependent, and the most that one can say is that a density dependence of the form of Ref. [6] is not ruled out. (On the other hand, the simple model of $\eta = 1$, corresponding to vanishing pairing in the nuclear interior, is quite incompatible with the mass data.) Using these two forces, complete mass tables, referred to as HFB-2 [3] and HFB-3 [4], respectively, were constructed, including all the 9200 nuclei lying between the two drip lines over the range of Z and $N \geq 8$ and $Z \leq 120$.

This paper is the second in a series of studies of possible modifications to the original HFB-2 calculation [3], with respect to both the force model and the method of calculation. Our motivation for making such modifications is mainly astrophysical: see Section I of paper I of this series [4], in which we dealt with the question of the density dependence of the pairing force. The main purpose of the present paper is to examine the role of the effective nucleon mass in Skyrme-HFB mass formulas.

We begin by recalling that the HF equation, i.e., the equation determining the s.p. states, has for the Skyrme forces (1) and our choice of symmetries the particularly simple form

$$\left\{ -\nabla \cdot \frac{\hbar^2}{2M_q^*(\mathbf{r})} \nabla + U_q(\mathbf{r}) + V_q^{coul}(\mathbf{r}) - i\mathbf{W}_q(\mathbf{r}) \cdot \nabla \times \boldsymbol{\sigma} \right\} \phi_{i,q} = \epsilon_{i,q} \phi_{i,q}. \quad (5)$$

All quantities appearing here are defined as in, for example, Ref. [7], but the essential point is that all the non-locality is confined to the effective mass $M_q^*(\mathbf{r})$, which is given in terms of the Skyrme parameters by

$$\frac{\hbar^2}{2M_q^*(\mathbf{r})} = \frac{\hbar^2}{2M} + \frac{1}{8} \{ t_1(2+x_1) + t_2(2+x_2) \} \rho(\mathbf{r}) + \frac{1}{8} \{ t_2(2x_2+1) - t_1(2x_1+1) \} \rho_q(\mathbf{r}), \quad (6)$$

the subscript q denoting neutron or proton. At any point in the nucleus the two effective masses $M_n^*(\mathbf{r})$ and $M_p^*(\mathbf{r})$ are now seen to be determined entirely by the local densities according to

$$\frac{\hbar^2}{2M_q^*} = \frac{2\rho_q}{\rho} \frac{\hbar^2}{2M_s^*} + \left(1 - \frac{2\rho_q}{\rho} \right) \frac{\hbar^2}{2M_v^*}, \quad (7)$$

where M_s^* and M_v^* are the so-called isoscalar and isovector effective masses, respectively, quantities that are determined by the Skyrme-force parameters according to

$$\frac{\hbar^2}{2M_s^*} = \frac{\hbar^2}{2M} + \frac{1}{16} \{ 3t_1 + t_2(5+4x_2) \} \rho, \quad (8a)$$

and

$$\frac{\hbar^2}{2M_v^*} = \frac{\hbar^2}{2M} + \frac{1}{8} \{ t_1(2+x_1) + t_2(2+x_2) \} \rho. \quad (8b)$$

The single-particle energies $\epsilon_{i,q}$ of even nuclei, obtained as eigenvalues of the HF Hamiltonian, Eq. (5), are often identified with the one-nucleon separation energies into or from certain low-lying excited states in adjacent odd- A nuclei, see [8] and references therein. It is known that to have the same density of s.p. levels $\epsilon_{i,q}$ in the vicinity of the Fermi level as observed in experiment for heavy and intermediate-mass nuclei, one must have M_s^*/M equal to, or close to, 1.0 at saturation density ρ_0 [9, 10] (we see from Eq. (7) that the isovector effective mass M_v^* will have little influence on s.p. energies of nuclei that are relatively close to the stability line). On the other hand, INM calculations with forces that are realistic in the sense that they fit the two- and three-nucleon data (and therefore require an explicit treatment of the short-range correlations that are built in an effective way into the forces for HFB calculations) indicate that M_s^*/M lies in the range 0.6–0.9 for $\rho = \rho_0$ [11, 12, 13, 14, 15]. Rough experimental confirmation that M_s^* is indeed significantly smaller than M came first from measurements of the deepest s.p. states in light nuclei [16] (the deepest s.p. states of heavier nuclei have not been measured); see Refs. [17, 18, 19] for theoretical discussions. More precise empirical information comes from analyses of the giant isoscalar quadrupole resonance, which lead to a value of around $0.8M$ for M_s^* at $\rho = \rho_0$, according to Ref. [20].

Actually, there is no contradiction between these two sets of values of M_s^*/M , since Refs. [21, 22] have shown that in finite nuclei one can obtain reasonable s.p. level densities near the Fermi level with the INM values of M_s^*/M , i.e., of 0.6–0.9, provided one takes into account the coupling between s.p. excitation modes and surface-vibration RPA modes. Since the good agreement with measured s.p. level densities found in Ref. [10] was obtained without making these corrections it must be supposed that the resulting error is being compensated by the higher value of M_s^*/M , i.e., $M_s^*/M \simeq 1.0$, which may thus be regarded as a phenomenological value that

leads to good agreement with measured s.p. energies in straightforward HF, or other mean-field calculations, without any of the complications of Refs. [21, 22].

Now the fact that in all our previous mass fits [1, 2, 3, 4], where no constraints were placed on the effective mass, we found $M_s^*/M \simeq 1.0$ at the density $\rho = \rho_0$ suggests that obtaining a correct s.p. spectrum in the vicinity of the Fermi level is a necessary condition for an optimum mass fit. This conclusion tends to be confirmed by the occupation-number representation of the Strutinsky theorem, which approximates the total energy of the nucleus as

$$E \simeq \tilde{E} + \sum_i \epsilon_i \delta n_i , \quad (9)$$

where \tilde{E} is a smoothed, average value of E , while $\delta n_i = n_i - \tilde{n}_i$, in which n_i is the actual occupation number of the s.p. state i and \tilde{n}_i is an average occupation number, given by, for example, Eq. (IV.18) of the review of Brack *et al.* [23]. But in Section IV.6 of this same paper [23] it is shown that δn_i is non-vanishing only for s.p. states lying within about $20A^{-1/3}$ MeV of the Fermi level. We may expect that it will be difficult to obtain correct masses if the s.p. spectrum over this interval is not reproduced, and it is quite comprehensible that the optimal mass fits published so far require that M_s^*/M take a value close to 1.0 at the density $\rho = \rho_0$. Indeed, with a Skyrme force of the form (1) and density-independent δ -function pairing forces treated within the BCS approximation, Farine *et al.* [24] found that if M_s^*/M was constrained to be equal to 0.8 then in fitting 416 quasi-spherical nuclei it was impossible to reduce the rms error below 1.141 MeV (parameter set MSk5*). On the other hand, when the constraint on M_s^*/M was released the rms error for the same data set fell to 0.709 MeV, M_s^*/M rising to 1.05 (parameter set MSk5). Moreover, the Skyrme force SLy4 [25] with $M_s^*/M = 0.7$ does not reproduce very well the masses of the few open-shell nuclei considered (see Figs. 1–4 of Ref. [25]).

Nevertheless, there remains some room for maneuver in Eq. (9), since shifts in the s.p. energies ϵ_i resulting from a change in the effective mass could in principle be compensated by appropriate changes in the δn_i , provided full use was made of all the degrees of freedom in the force, with particular emphasis on those that have not hitherto been exploited; of especial interest in this respect is the pairing cutoff, which, for example, was fixed at the same value in the MSk5 and MSk5* fits ($41 A^{-1/3}$ MeV into the continuum). In the present paper we pursue these possibilities with the aim of seeing to what extent it is possible to maintain quality mass fits with lower values of M_s^*/M , more appropriate to INM. Part of our own interest in this question lies in our search for a unique effective interaction suitable for the determination of an equation of state describing the formation of nuclear matter from isolated finite nuclei that occurs during stellar collapse [24, 26]. A lower value of M_s^*/M , corresponding to INM, will certainly be appropriate in the final stage;

the question here is to see to what extent such a choice of M_s^*/M can suitably describe the isolated nuclei prevailing at the beginning of the collapse. (Similar considerations will arise in the more or less inverse sequence of events traced out during the neutron-matter decompression that occurs, for example, in the aftermath of neutron-star mergers.)

In this paper we also replace our original approximate correction for the centre-of-mass motion by a much improved treatment, and we describe this first, in Section II, leaving until Section III the discussion of the role of the effective mass. There, two different values of M_s^* at the density $\rho = \rho_0$, $0.92M$ and $0.8M$, will be considered, and four new mass tables, HFB-4, HFB-5, HFB-6, and HFB-7, generated, each value of M_s^* being calculated with and without a density dependence in the pairing force.

II. CENTER-OF-MASS CORRECTION

Mean-field approaches like HF or HFB, which establish an intrinsic frame of the nucleus, break several symmetries of the Hamiltonian and the wave function in the laboratory frame [8, 27]. For example, finite nuclei break translational invariance, deformed nuclei are not rotational invariant, and the HFB approach breaks particle-number symmetry. Doing so adds desired correlations to the modeling – as multi-particle-multi-hole states associated with deformation, pairing, etc. – but at the same time gives rise to an admixture of excited states to the calculated ground state. Their spurious contribution to the total mass changes with nucleon numbers and deformation. The energy of those spurious modes, which are not explicitly removed from the calculated ground state, will be simulated by the Skyrme force through the parameter fit, which might spoil the properties of the resulting forces [29].

A rigorous way to restore the broken symmetries is projection on exact quantum numbers, but this would be too time-consuming to be used for the large-scale mass fits performed here. A simpler procedure is to estimate the contribution to the binding energy in a suitable approximation, and to add the resulting corrections to the calculated masses; such a procedure has already been adopted by many workers for the center-of-mass (cm) correction, the rotational correction, and the Lipkin-Nogami correction to the pairing energy. In our own HF mass formulas [1, 2, 3, 4] we have used such a procedure for the c.m. and rotational corrections, as described in Ref. [7]. In the present paper we improve our treatment of the cm correction, as discussed below in this section, but otherwise the Skyrme-HFB formalism used here is essentially as described in detail in our first HFB paper [2]. In particular, we have not yet made any correction for particle-number fluctuations; this will be the topic of a forthcoming paper.

The HFB ground state is not an eigenstate of the total momentum operator. Thus, although the expectation value of the momentum operator $\hat{\mathbf{P}} \equiv \sum_i \hat{\mathbf{p}}_i$

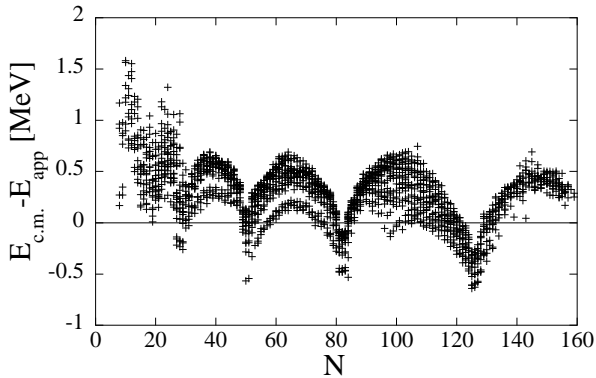


FIG. 1: Comparison for the 2135 nuclei included in the 2001 mass compilation of [5] of the binding energies obtained with the improved centre-of-mass correction E_{cm} with those obtained with the approximation of [28] E_{app} . Both calculations use the BSk2 Skyrme force and are made in the spherical approximation.

in the cm frame $\langle \text{HFB} | \hat{\mathbf{P}} | \text{HFB} \rangle$ vanishes, its dispersion $\langle \text{HFB} | \hat{\mathbf{P}}^2 | \text{HFB} \rangle$ does not. Gaussian overlap approximation to exact momentum projection gives for the spurious cm energy

$$E_{cm} = \frac{1}{2MA} \langle \text{HFB} | \hat{\mathbf{P}}^2 | \text{HFB} \rangle, \quad (10)$$

which has to be subtracted from the calculated total energy. To avoid the time-consuming evaluation of the non-diagonal terms $\hat{\mathbf{p}}_i \cdot \hat{\mathbf{p}}_j, i \neq j$, in the past we have always adopted the approximation of Butler *et al.* [28], which takes explicit account only of the diagonal terms, thus

$$E_{cm} \simeq \frac{f(A)}{2MA} \langle \text{HFB} | \sum_i \hat{\mathbf{p}}_i^2 | \text{HFB} \rangle, \quad (11)$$

where $f(A)$ is a simple function that makes this expression exact in the case of pure oscillator s.p. states. From now on, we evaluate the cm correction according to Eq. (10), doing so, however, perturbatively. That is, both the diagonal and off-diagonal terms of Eq. (10) are included only in the calculation of the converged total energy, not in the variational equation that leads to the mean field in the HF equation (5).

The effect of this improved treatment is seen in Fig. 1, where for each of the 2135 nuclei of known mass we show the difference between the total energy calculated with our new method, and that calculated with the approximation of Ref. [28]. The force used for this comparison is BSk2, and for simplicity we assume a spherical configuration for all nuclei. The differences are largest for light nuclei, for which they can reach 1.5 MeV; strong shell effects will be noticed.

Of course, in fitting force BSk2 to the mass data these errors in the approximation of Ref. [28] were absorbed to some extent into the force parameters. It would be interesting to refit the BSk2 force to the same data using the improved cm correction, and compare the new

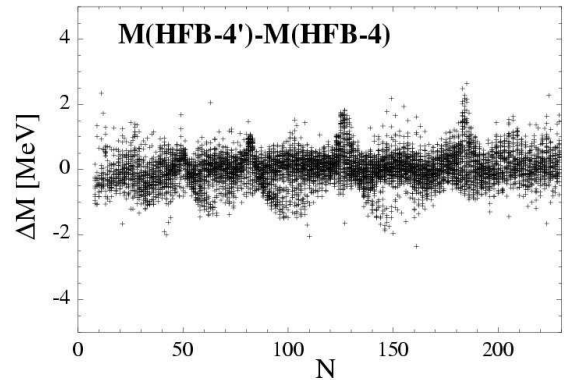


FIG. 2: Differences between the HFB-4' and HFB-4 masses as a function of the neutron number N for all nuclei with $Z, N \geq 8$ lying between the proton and neutron driplines up to $Z = 120$.

with the original BSk2 fit. For practical reasons, we make this comparison on the basis of the force BSk4, described in the next section. This force (like the forces BSk5, BSk6 and BSk7) is calculated with the improved cm correction [29], so we refit the force BSk4 to the data using the approximate cm correction of Ref. [28], defining thereby the force BSk4'. We find that the change in the rms error of the fit is negligible, going from 0.680 to 0.681 MeV. The mass differences between the corresponding BSk4' and BSk4 predictions are compared in Fig. 2 for all nuclei with $Z, N \geq 8$ lying between the proton and neutron driplines up to $Z = 120$. In contrast to Fig. 1, deformation effects are taken into account consistently. The difference in the shell structure between the improved treatment of the cm correction [29] and the approximation of Ref. [28], as seen in Fig. 1, is still present after renormalizing the Skyrme forces on experimental masses. The mass differences remain however smaller than 2 MeV, even for exotic neutron-rich or superheavy nuclei.

III. CHOICE OF THE ISOSCALAR EFFECTIVE MASS, AND THE NEW HFB MASS TABLES

Most INM calculations of M_s^* at the density $\rho = \rho_0$ give a value of around $0.8M$, the most recent such calculation being that of Ref. [15]. On the other hand, using the so-called extended Brueckner-Hartree-Fock method with realistic nucleonic forces, Ref. [14] finds $0.92M$. Rather than attempt to decide between these two values we shall here consider both of them, with the value of $0.92M$ being imposed on parameter sets BSk4 and BSk5 (mass formulas HFB-4 and HFB-5, respectively), and the value of $0.8M$ being imposed on parameter sets BSk6 and BSk7 (mass formulas HFB-6 and HFB-7, respectively). The pairing force in both BSk4 and BSk6 is supposed to be density-independent, while that of BSk5 and BSk7

TABLE I: Rms (σ) and mean ($\bar{\epsilon}$) errors (in MeV) in the predictions of masses M obtained with the BSk2–7 forces. Also given are the model standard deviation and the model mean error (see text for more details) on the set of all 2135 measured masses, on the 928 stable and neutron-rich nuclei, and on the 1207 proton-rich nuclei. The last two lines correspond to the rms and mean errors (in fm) for the predictions of the 523 measured charge radii (r_c).

	BSk2	BSk3	BSk4	BSk5	BSk6	BSk7
$\sigma(M)$ (2135 nuclei)	0.674	0.656	0.680	0.675	0.686	0.676
$\bar{\epsilon}(M)$ (2135 nuclei)	0.000	-0.006	-0.115	-0.005	-0.013	-0.004
$\sigma_{mod}(M)$ (2135 nuclei)	0.660	0.639	0.661	0.655	0.666	0.658
$\bar{\epsilon}_{mod}(M)$ (2135 nuclei)	-0.007	-0.015	0.106	-0.006	0.013	0.026
$\sigma_{mod}(M)$ (928 nuclei)	0.709	0.709	0.678	0.685	0.713	0.707
$\bar{\epsilon}_{mod}(M)$ (928 nuclei)	-0.168	-0.118	0.001	-0.122	0.093	-0.085
$\sigma_{mod}(M)$ (1207 nuclei)	0.620	0.581	0.649	0.631	0.629	0.618
$\bar{\epsilon}_{mod}(M)$ (1207 nuclei)	0.113	0.062	0.186	0.080	0.092	0.109
$\sigma(r_c)$ (523 nuclei)	0.0282	0.0291	0.0282	0.0270	0.0262	0.0260
$\bar{\epsilon}(r_c)$ (523 nuclei)	0.0138	0.0161	-0.0115	0.0104	0.0028	-0.0030

TABLE II: Skyrme-force and pairing-force parameters of BSk2–BSk7

	BSk2	BSk3	BSk4	BSk5	BSk6	BSk7
t_0 [MeV fm ³]	-1790.6248	-1755.1297	-1776.9376	-1778.8934	-2043.3174	-2044.2484
t_1 [MeV fm ⁵]	260.996	233.262	306.884	312.727	382.127	385.973
t_2 [MeV fm ⁵]	-147.167	-135.284	-105.670	-102.883	-173.879	-131.525
t_3 [MeV fm ^{3+3γ}]	13215.1	13543.2	12302.1	12318.37	12511.7	12518.8
x_0	0.498986	0.476585	0.542594	0.444510	0.735859	0.729193
x_1	-0.089752	-0.032567	-0.535165	-0.488716	-0.799153	-0.932335
x_2	0.224411	0.470393	0.494738	0.584590	-0.358983	-0.050127
x_3	0.515675	0.422501	0.759028	0.569304	1.234779	.236280
W_0 [MeV fm ⁵]	119.047	116.07	129.50	130.70	142.38	146.93
γ	0.343295	0.361194	1/3	1/3	1/4	1/4
V_n^+ [MeV fm ³]	-238	-359	-273	-429	-321	-505
V_n^- [MeV fm ³]	-265	-407	-289	-463	-325	-514
V_p^+ [MeV fm ³]	-247	-365	-285	-447	-338	-531
V_p^- [MeV fm ³]	-278	-413	-302	-483	-341	-541
η	0	0.45	0	0.45	0	0.45
α	0	0.47	0	0.47	0	0.47
ϵ_A [MeV]	15	14	16	16	17	17
V_W [MeV]	-2.05	-2.05	-1.72	-1.96	1.76	1.86
λ	485	460	740	480	700	720
V'_W [MeV]	0.70	0.54	0.54	0.50	0.58	0.54
A_0	28	30	30	30	28	28

is taken to have a density dependence of the form (2), with the parameters η and α taking the values given by Garrido *et al.* [6], as with the BSk3 force [4]. In all four cases the isovector mass at $\rho = \rho_0$ is left unconstrained in the fits.

We fit all four of these forces to the same data set as the one to which BSk2 [3] and BSk3 [4] were fitted, i.e., the 2135 nuclei with $Z, N \geq 8$ whose masses have been measured and compiled in the 2001 AME [5]. As in the fits of BSk2 and BSk3, we impose a lower limit on the INM symmetry coefficient J , in order to prevent the collapse of neutron matter at nuclear densities, as

required by the observed stability of neutron stars. In the case of BSk5, we use the INM calculation of [14] to constrain not only the effective mass to $0.92M$, but also the symmetry coefficient to $J = 28.7$ MeV. Also, we set the equilibrium density of symmetric INM at $\rho_0 = 0.1575$ fm⁻³, it having been found that this ensures very good predictions for rms charge radii along with near-optimal mass fits.

From the first line of Table I we see that while forces BSk2 and BSk3, in which M_s^* is unconstrained, still give the best fits, all four of the new forces, BSk4–7, give fits that are almost as good, the deterioration on constraining

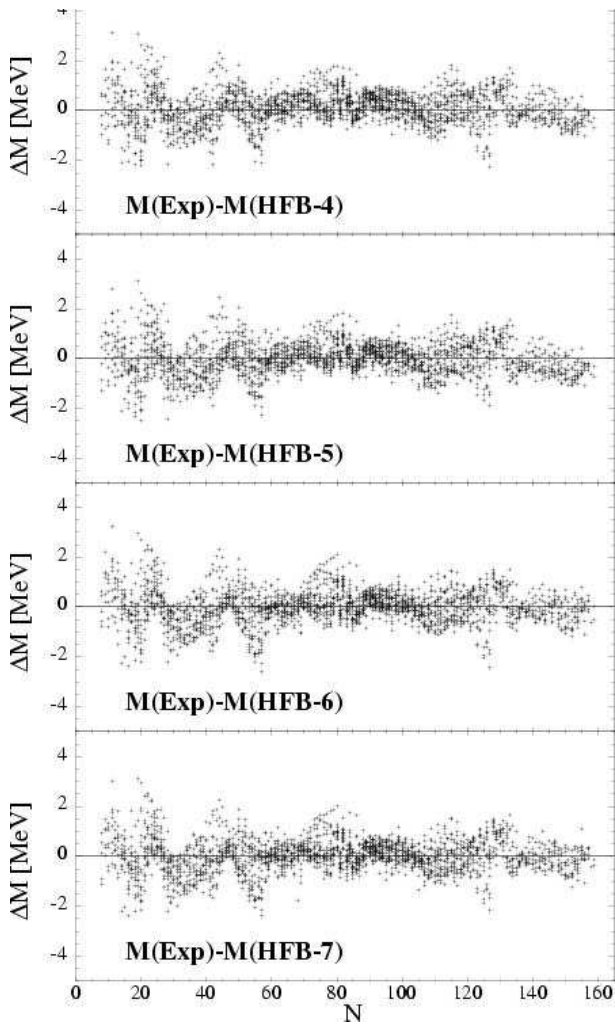


FIG. 3: Differences between experimental and calculated mass excesses as a function of the neutron number N for the HFB-4 to HFB-7 mass tables.

M_s^* being quite negligible. Fig. 3 displays the deviations of the calculated masses from the experimental values.

Table I also has entries for a “model standard deviation” σ_{mod} and a “model mean error” $\bar{\epsilon}_{mod}$. These quantities have been introduced [30, 31] as an improved measure of the validity of the physical model that is being fitted to the data, the standard rms error σ suffering from the defect that it does not take account of the experimental errors of the individual mass measurements, as given by Audi and Wapstra [5, 32]. The standard rms error is a legitimate measure when the experimental errors are small compared to the rms error itself, but some of the most recent measurements of nuclei far from the stability line have errors in excess of 1 MeV [5]. In such cases, σ_{mod} and $\bar{\epsilon}_{mod}$ give a better assessment of the validity of a given mass formula, since they weight each data point in terms of its experimental error, following a procedure based on the method of maximum likelihood [30, 31]. The definition of σ_{mod} that we adopt is that of Eqns.

(42) and (43) of Ref. [30] (which writes σ_{mod} as σ_{th}^*), while our definition of $\bar{\epsilon}_{mod}$ is that of Eqns. (9) and (10) of Ref. [31] (which writes $\bar{\epsilon}_{mod}$ as μ_{th}^*); for a discussion of the relationship between the ways in which the two papers [30] and [31] treat model errors see Appendix B of Ref. [33]. We show σ_{mod} and $\bar{\epsilon}_{mod}$ for the full data set of 2135 masses to which the fit was made, as well as to the two subsets of 1207 proton-rich nuclei and 928 stable and neutron-rich nuclei. None of these model errors suggests that any particular force is significantly better or worse than any of the others, as far as masses are concerned. The fact that mass fits with values of M_s^*/M constrained to be equal to 0.8 can be obtained which are almost as good as those for which M_s^*/M is unconstrained (always emerging with a value close to 1.0) is, we have found, essentially a consequence of our exploitation of the degree of freedom associated with the pairing cutoff, a reduction in M_s^*/M being almost completely compensated by an increase in the parameter ε_Λ appearing in Eq. (4) (see Table II).

We also show in Table I the rms and mean deviations between our calculated and experimental charge radii for the 523 nuclei listed in the 1994 compilation [34] (for more details on the HFB derivation of the charge radii, see Ref. [35]). The overall agreement with experiment is seen to be excellent. However, none of the forces is able to completely reproduce the much discussed kink in the Pb isotope chain at $N = 126$.

The parameters of the forces BSk2–7 are given in Table II, while the corresponding macroscopic parameters, i.e., the parameters relating to INM and SINM (semi-infinite nuclear matter) calculated for all these forces, are shown in Table III. The quantities appearing in this latter table that have not yet been defined are: a_v , the energy per nucleon at equilibrium in symmetric INM; K_v , the INM incompressibility; G_0 and G'_0 , the Landau parameters defined in Ref. [36]; ρ_{frm} , the density at which neutron matter flips over into a ferromagnetic state that has no energy minimum and would collapse indefinitely [37]; a_{sf} , the surface coefficient; and Q , the surface-stiffness coefficient [38]. It will be recalled that

TABLE III: Macroscopic parameters of the forces BSk2–BSk7

	BSk2	BSk3	BSk4	BSk5	BSk6	BSk7
a_v [MeV]	-15.794	-15.804	-15.773	-15.802	-15.749	-15.760
ρ_0 [fm^{-3}]	0.1575	0.1575	0.1575	0.1575	0.1575	0.1575
J [MeV]	28.0	27.9	28.0	28.7	28.0	28.0
M_s^*/M	1.04	1.12	0.92	0.92	0.80	0.80
M_v^*/M	0.86	0.89	0.85	0.84	0.86	0.87
K_v [MeV]	233.6	234.8	236.8	237.2	229.1	229.3
G_0	-0.705	-0.994	-0.478	-0.579	0.065	-0.101
G'_0	0.446	0.497	0.457	0.454	0.312	0.356
ρ_{frm}/ρ_0	1.1	1.00	1.30	1.20	1.81	1.62
a_{sf} [MeV]	17.5	17.5	17.3	17.5	17.2	17.3
Q [MeV]	68	67	76	52	83	80

in all cases the values of ρ_0 and J were imposed, as were the values of M_s^*/M . On the other hand, M_v^*/M is unconstrained, but it is gratifying to note that for all fits its value comes out to be quite close to the value of 0.83 that we infer from the INM calculations of Zuo *et al.* [14] (see especially their Fig. 9). Nevertheless, a word of caution is necessary here, since it is known from Ref. [39] that the rms error of the mass fit varies only slowly with M_v^* . As for K_v , all our forces give values falling within the experimental range of 225–240 MeV established by Youngblood *et al.* [40]. All our forces likewise satisfy the condition G_0 and $G'_0 > -1$ for stability against spin and spin-isospin flips [41] at saturation density. Finally, it will be seen that reducing M_s^* seems to assure greater stability to neutron matter against ferromagnetic flips. For the values of ρ_{frmg} , G_0 and G'_0 given in Table III, it is assumed that the effective spin-spin interaction is obtained from the exchange terms of the two-body Skyrme force, eq. (1). There is another possible view of the effective Skyrme interaction, see [8, 42] and references given therein, which leaves the coupling constants that determine ρ_{frmg} , G_0 and G'_0 as additional free parameters not constrained by our current mass fit.

Neutron Matter. All our present forces have a value of $J \simeq 28$ MeV (except BSk5 with $J = 28.7$ MeV) which was actually set as a lower limit in the search on the Skyrme parameters. It is possible that a slightly better mass fit could have been obtained with a value somewhat closer to 27.5 MeV, but this might have engendered an unphysical collapse of neutron matter at nuclear densities. The situation in neutron matter for our forces is as shown in Fig. 4; the solid curve labeled FP shows the results of Friedman and Pandharipande [12] for the realistic force Argonne v14 + TNI, containing two- and three-nucleon terms. More recent realistic calculations of neutron matter [43, 44, 45] give similar results up to nuclear densities. At low densities, all forces give the same predictions. At densities higher than the nuclear density, where the validity of the non-relativistic approach followed here could admittedly be questioned, the new

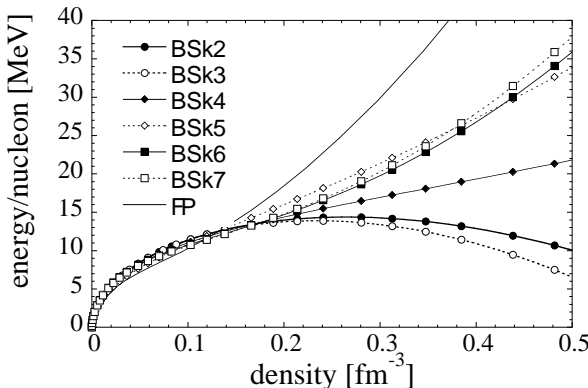


FIG. 4: Energy-density curves of neutron matter for the forces of this paper, and for the calculations of Ref. [12] (FP).

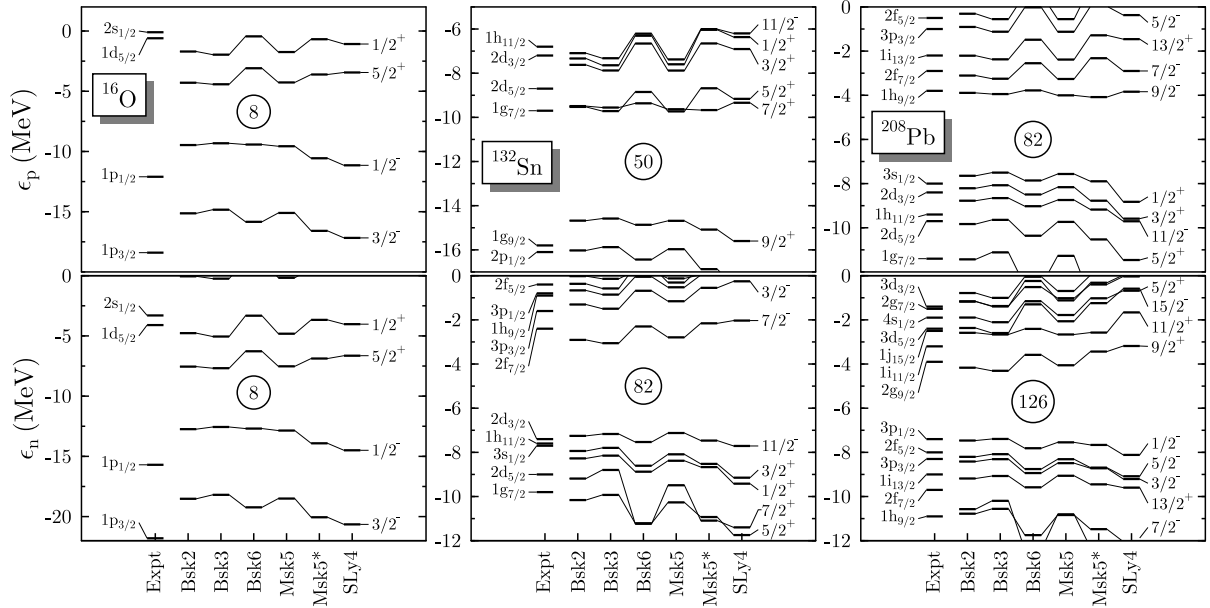
TABLE IV: Single-particle proton levels in ^{208}Pb (MeV). Experimental values are taken from Ref. [17]. The asterisk denotes the Fermi level. The quantity Δ_p is the interval between the centroids of the $1g$ and $2f$ doublets.

Level	BSk2	BSk3	BSk6	MSk5	MSk5*	SLy4	Expt.
$1s_{1/2}$	-33.1	-31.4	-38.9	-31.8	-40.5	-44.0	-
...
$1g_{9/2}$	-14.8	-14.4	-16.2	-14.6	-16.7	-17.7	-15.4
$1g_{7/2}$	-11.4	-11.1	-12.6	-11.3	-13.1	-13.5	-11.4
$2d_{5/2}$	-9.8	-9.6	-10.4	-9.7	-10.5	-11.5	-9.7
$1h_{11/2}$	-8.8	-8.7	-9.0	-8.7	-9.2	-9.7	-9.4
$2d_{3/2}$	-8.2	-8.1	-8.5	-8.2	-8.8	-9.6	-8.4
$3s_{1/2}^*$	-7.6	-7.5	-7.9	-7.6	-7.9	-8.8	-8.0
$1h_{9/2}$	-3.9	-3.9	-3.8	-4.0	-4.1	-3.8	-3.8
$2f_{7/2}$	-3.1	-3.3	-2.6	-3.3	-2.3	-2.9	-2.9
$1i_{13/2}$	-2.2	-2.4	-1.5	-2.4	-1.3	-1.5	-2.2
$3p_{3/2}$	-0.3	-0.6	0.6	-0.6	0.9	0.4	-1.0
$2f_{5/2}$	-0.9	-1.1	0.0	-1.1	0.0	-0.4	-0.5
Δ_p	11.0	10.5	13.1	10.7	13.9	14.0	11.7

TABLE V: Single-particle neutron levels in ^{208}Pb (MeV). Experimental values are taken from Ref. [17]. The asterisk denotes the Fermi level. The quantity Δ_n is the interval between the centroids of the $2f$ and $3d$ doublets.

Level	BSk2	BSk3	BSk6	MSk5	MSk5*	SLy4	Expt.
$1s_{1/2}$	-39.5	-36.9	-51.5	-40.7	-49.9	-57.9	-
...
$1h_{9/2}$	-10.6	-10.2	-12.4	-10.8	-12.3	-12.5	-10.9
$2f_{7/2}$	-10.8	-10.6	-11.7	-10.8	-11.5	-12.0	-9.7
$1i_{13/2}$	-9.2	-9.1	-9.6	-9.1	-9.4	-9.6	-9.0
$3p_{3/2}$	-8.4	-8.3	-8.9	-8.5	-8.7	-9.2	-8.3
$2f_{5/2}$	-8.2	-8.1	-8.8	-8.3	-8.7	-9.1	-8.0
$3p_{1/2}^*$	-7.5	-7.4	-7.8	-7.6	-7.7	-8.1	-7.4
$2g_{9/2}$	-4.2	-4.3	-3.6	-4.1	-3.4	-3.2	-3.9
$1i_{11/2}$	-2.6	-2.7	-2.4	-2.7	-2.6	-1.7	-3.2
$-1j_{15/2}$	-2.4	-2.6	-1.3	-2.1	-1.2	-0.6	-2.5
$3d_{5/2}$	-1.9	-2.1	-1.2	-1.8	-1.0	-0.7	-2.4
$4s_{1/2}$	-1.2	-1.4	-0.6	-1.0	-0.3	0.0	-1.9
$2g_{7/2}$	-1.2	-1.4	-0.2	-1.1	-0.3	0.0	-1.5
$3d_{3/2}$	-0.8	-1.0	0.0	-0.7	0.1	0.3	-1.4
Δ_n	8.2	7.8	9.8	8.3	9.7	10.5	7.2

forces are found to lead to harder neutron-matter curves and avoid the collapse obtained for BSk2. In particular, BSk5 with $J = 28.7$ MeV gives very similar energies per nucleon as BSk6 and BSk7 with $J = 28$ MeV due to the much lower value of the x_1 parameter reached by the mass fit (see Table II).

FIG. 5: Single-particle spectra for ^{16}O , ^{132}Sn , and ^{208}Pb .

Single-particle spectra. Clearly, it is of interest to see what happens to the s.p. energies when the effective mass is reduced while maintaining a very good fit to the masses. In Tables IV – IX and Figure 5 we show the s.p. spectra of ^{208}Pb , ^{132}Sn , and ^{16}O for forces BSk2, BSk3, and BSk6, along with those of the old forces MSk5, MSk5* and SLy4. Comparing BSk2 and BSk3 shows that making the pairing density-dependent has little effect on the s.p. energies. Also, the spectra of BSk2 and MSk5 are very similar, but different from those of BSk6, MSk5*, and SLy4, which, however, resemble each other quite closely. That is, the effective mass still determines the s.p. spectra. But while BSk2 and BSk6 have different s.p. spectra they give very similar fits to the mass data.

TABLE VI: Single-particle proton levels in ^{132}Sn (MeV). Experimental values are taken from Refs. [46, 47]. The asterisk denotes the Fermi level. The quantity Δ_p is the interval between the centroids of the $1g$ and $2d$ doublets.

Level	BSk2	BSk3	BSk6	MSk5	MSk5*	SLy4	Expt.
$1s_{1/2}$	-38.7	-37.1	-44.2	-37.5	-48.1	-49.0	–
...
$2p_{1/2}$	-16.0	-15.9	-16.4	-15.9	-18.7	-17.6	-16.1
$1g_{9/2}^*$	-14.7	-14.6	-14.9	-14.7	-16.6	-15.6	-15.8
$1g_{7/2}$	-9.5	-9.6	-9.4	-9.6	-11.1	-9.3	-9.7
$2d_{5/2}$	-9.5	-9.7	-8.9	-9.7	-10.9	-9.2	-8.7
$2d_{3/2}$	-7.6	-7.9	-6.7	-7.9	-8.5	-6.9	-7.2
$3s_{1/2}$	-7.3	-7.6	-6.3	-7.6	-8.7	-6.4	–
$1h_{11/2}$	-7.1	-7.3	-6.2	-7.4	-7.5	-6.2	-6.8
Δ_p	3.7	3.4	4.5	3.7	4.3	4.5	5.1

On the other hand, the s.p. spectra of BSk6 are very similar to those of MSk5*, but the latter gives a much worse mass fit. The only way in which we can reconcile this behavior with the Strutinsky theorem in the form (9) is to invoke the δn_i quantities: shifts in the δn_i compensate the differences between the s.p. spectra of BSk2 and BSk6, and at the same time account for the different mass predictions of BSk6 and MSk5*, despite their similar s.p. spectra. This interpretation in terms of the occupation numbers is strengthened by the fact that the decoupling

TABLE VII: Single-particle neutron levels in ^{132}Sn (MeV). Experimental values are taken from Ref. [47]. The asterisk denotes the Fermi level. The quantity Δ_n is the interval between the centroids of the $2d$ and $3p$ doublets.

Level	BSk2	BSk3	BSk6	MSk5	MSk5*	SLy4	Expt.
$1s_{1/2}$	-37.8	-35.3	-49.8	-39.0	-48.1	-55.8	–
...
$1g_{7/2}$	-9.2	-8.8	-11.2	-9.5	-11.1	-11.4	-9.8
$2d_{5/2}$	-10.2	-9.9	-11.2	-10.3	-10.9	-11.7	-9.0
$3s_{1/2}$	-8.3	-8.1	-8.9	-8.4	-8.7	-9.4	-7.7
$1h_{11/2}$	-7.3	-7.2	-7.5	-7.1	-7.5	-7.7	-7.6
$2d_{3/2}^*$	-7.9	-7.8	-8.6	-8.0	-8.5	-9.1	-7.4
$2f_{7/2}$	-2.9	-3.1	-2.3	-2.8	-2.2	-2.0	-2.4
$3p_{3/2}$	-1.3	-1.5	-0.7	-1.2	-0.5	-0.3	-1.6
$1h_{9/2}$	0.0	-0.1	0.2	-0.1	0.1	0.8	-0.9
$3p_{1/2}$	-0.7	-0.9	0.0	-0.5	0.1	0.3	-0.8
$2f_{5/2}$	-0.4	-0.6	0.4	-0.3	0.4	0.6	-0.4
Δ_n	8.2	7.8	9.7	8.4	9.6	10.6	7.1

TABLE VIII: Single-particle proton levels in ^{16}O (MeV). Experimental values are taken from Ref. [17]. The asterisk denotes the Fermi level. The quantity Δ_p is the interval between the centroid of the $1p$ doublet and the $2s_{1/2}$ state. (Errors in Table 6a of Ref. [24] for MSk5* corrected.)

Level	BSk2	BSk3	BSk6	MSk5	MSk5*	SLy4	Expt.
$1s_{1/2}$	-25.5	-24.5	-29.4	-25.4	-30.3	-32.9	-40 ± 8
$1p_{3/2}$	-15.1	-14.8	-15.8	-15.1	-16.6	-17.2	-18.4
$1p_{1/2}^*$	-9.5	-9.3	-9.4	-9.6	-10.6	-11.1	-12.1
$1d_{5/2}$	-4.3	-4.4	-3.1	-4.3	-3.6	-3.4	-0.6
$2s_{1/2}$	-1.7	-2.0	-0.4	-1.7	-0.7	-1.1	-0.1
Δ_p	11.5	11.0	13.2	11.6	13.9	14.1	16.2

TABLE IX: Single-particle neutron levels in ^{16}O (MeV). Experimental values are taken from Ref. [17]. The asterisk denotes the Fermi level. The quantity Δ_n is the interval between the centroid of the $1p$ doublet and the $2s_{1/2}$ state.

Level	BSk2	BSk3	BSk6	MSk5	MSk5*	SLy4	Expt.
$1s_{1/2}$	-28.9	-27.9	-33.0	-28.9	-33.9	-36.7	-
$1p_{3/2}$	-18.5	-18.2	-19.2	-18.5	-20.1	-20.7	-21.8
$1p_{1/2}^*$	-12.7	-12.6	-12.7	-12.9	-13.9	-14.5	-15.7
$1d_{5/2}$	-7.5	-7.7	-6.3	-7.5	-6.9	-6.6	-4.1
$2s_{1/2}$	-4.8	-5.1	-3.3	-4.8	-3.7	-4.0	-3.3
Δ_p	11.8	11.2	13.7	11.8	14.8	14.6	16.5

of the mass fits from the fits to the s.p. spectra is made possible only by adjustment of the pairing cutoff.

As for the agreement with the experimental s.p. spectra, we see that a value of M_s^*/M close to 1.0 is favored by the ^{208}Pb data, while ^{16}O favors a value of 0.8. The ^{132}Sn data are ambiguous, the neutron spectrum indicating the higher value of M_s^*/M , and the proton spectrum the lower value. Presumably, if we took into account the coupling of s.p. excitations and surface-vibration RPA modes for the forces with $M_s^*/M = 0.8$, as in Refs. [21, 22], the calculated s.p. spectra of heavy nuclei would be in better agreement with experiment, but we would then have to refit to the mass data.

Extrapolation to drip lines. With each of the forces BSk4–7 determined as described we constructed complete mass tables, labeled HFB-4 to HFB-7, respectively, for the same nuclei as were included in the HFB-2 and HFB-3 tables, i.e., all the 9200 nuclei lying between the two drip lines over the range of Z and $N \geq 8$ and $Z \leq 120$. The differences between the HFB-2 masses and the HFB-4, 5, 6, and 7 masses are displayed in Fig. 6 as a function

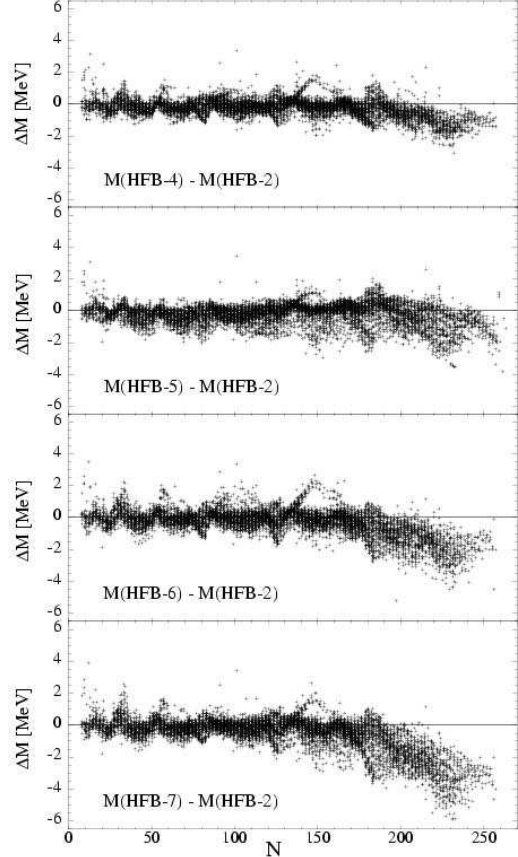


FIG. 6: Differences between the HFB-2 and HFB-4 to HFB-7 masses as a function of the neutron number N for all nuclei with $Z, N \geq 8$ lying between the proton and neutron driplines up to $Z = 120$.

of the neutron number N and in Fig. 7 as a function of the neutron separation energy S_n , where it will be seen that these differences never exceed 6 MeV, and even then only as the neutron drip line is approached, no matter what the value of Z (different published mass formulas all giving very good data fits can differ by up to 15 or 20 MeV at the drip lines [33]). Looking at the first and third panels of Fig. 6 shows that as M_s^*/M is reduced there is a definite tendency for open-shell nuclei to be bound a little more strongly, a trend that becomes more conspicuous for the heaviest nuclei. The second and last panels of this figure confirm the feature already noted in paper I [4] for density-dependent pairing: a similar tendency for open-shell nuclei to be more strongly bound, especially for the heaviest nuclei.

Actually, while differences of up to 6 MeV between the different mass predictions for nuclei far from the stability line may appear to be rather large, of far greater interest for practical applications such as to the r-process of nucleosynthesis are differential quantities such as the neutron separation energy S_n . For these quantities the differences between the different predictions are much smaller, as is

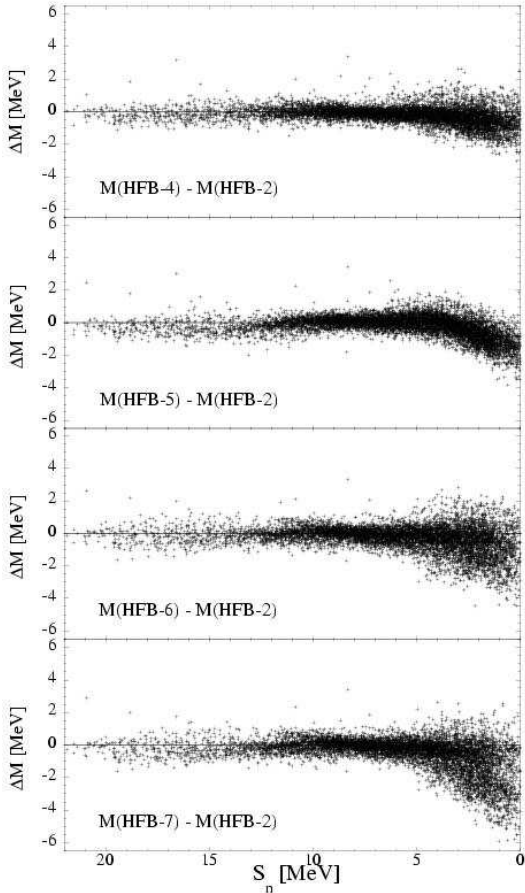


FIG. 7: Same as Fig. 6 as a function of the neutron separation energy S_n .

seen in Figs. 8 and 9, where we plot as a function of Z , for each of the magic numbers $N_0 = 50, 82, 126$, and 184 , respectively, the neutron-shell gaps, defined by

$$\begin{aligned} \Delta(N_0) &\equiv S_{2n}(Z, N_0) - S_{2n}(Z, N_0 + 2) \\ &= M(Z, N_0 - 2) + M(Z, N_0 + 2) - 2M(Z, N_0) \end{aligned} \quad (12)$$

calculated with BSk2, BSk4 and BSk6 (S_{2n} denotes the 2-neutron separation energy). From Figs. 8 and 9, it can be seen that the gaps do not depend significantly on the effective nucleon mass. The impact of such differences on the predicted r-process abundance distributions will be studied in more detail in a forthcoming paper.

For $N_0 = 50, 82$, and 126 , Figs. 8-9 show a strong disagreement with experiment for the new mass formulas in the vicinity of the (semi-) magic *proton* numbers $Z = 40, 50$, and 82 . This is related to the problem of “mutually supporting magicities” that we have already discussed in connection with the HFB-2 mass formula [3]. Clearly, it has not been solved, either by reducing the effective mass, or by introducing the shell-dependent cm correction. (We showed in paper I [4] that making the pairing density-dependent cannot help in this respect, either.)

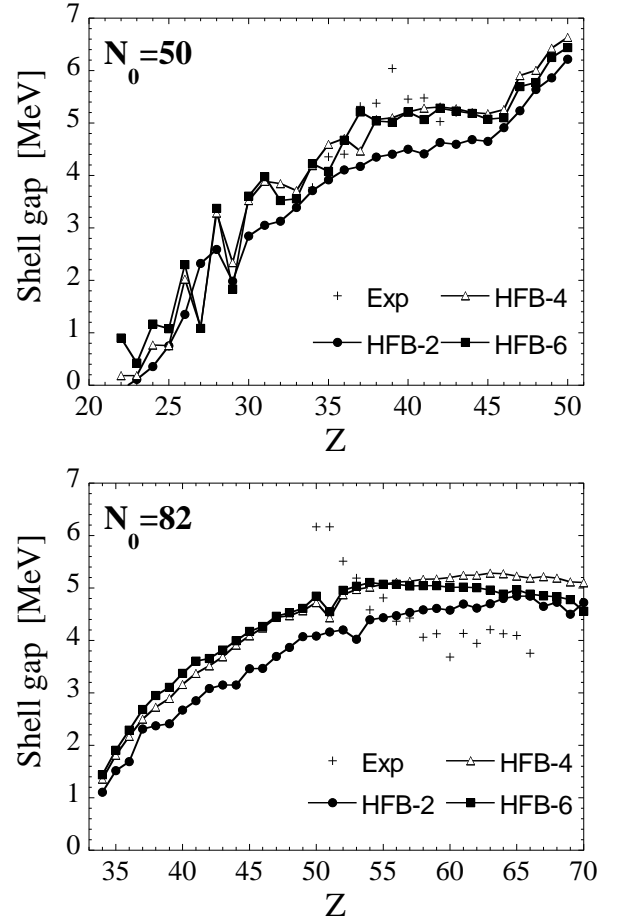


FIG. 8: $N_0 = 50$ (upper panel) and $N_0 = 82$ (lower panel) shell gap as a function of Z .

IV. CONCLUSIONS

Fitting Skyrme-type forces to the available mass data without any constraint on the effective mass always leads to an isoscalar effective mass M_s^* close to the real nucleon mass M . However, we have shown that we can reduce M_s^*/M to 0.8 without any significant reduction in the quality of the mass-data fit, although important changes in the s.p. spectra are thereby induced. This decoupling of the fit to the mass data from the fit to the s.p. data was made possible only by exploiting the pairing-force cutoff.

On this basis we constructed four new complete mass tables, referred to as HFB-4 to HFB-7, each one including all the 9200 nuclei lying between the two drip lines over the range of Z and $N \geq 8$ and $Z \leq 120$. HFB-4 and HFB-5 have M_s^*/M constrained to the value 0.92, with the former having a density-independent pairing, and the latter a density-dependent pairing. HFB-6 and HFB-7 are similar, except that M_s^*/M is constrained to 0.8. The mass-data fits are almost as good as those given by mass formulas HFB-2 and HFB-3, in which M_s^*/M was unconstrained. Actually, in these four new mass formulas

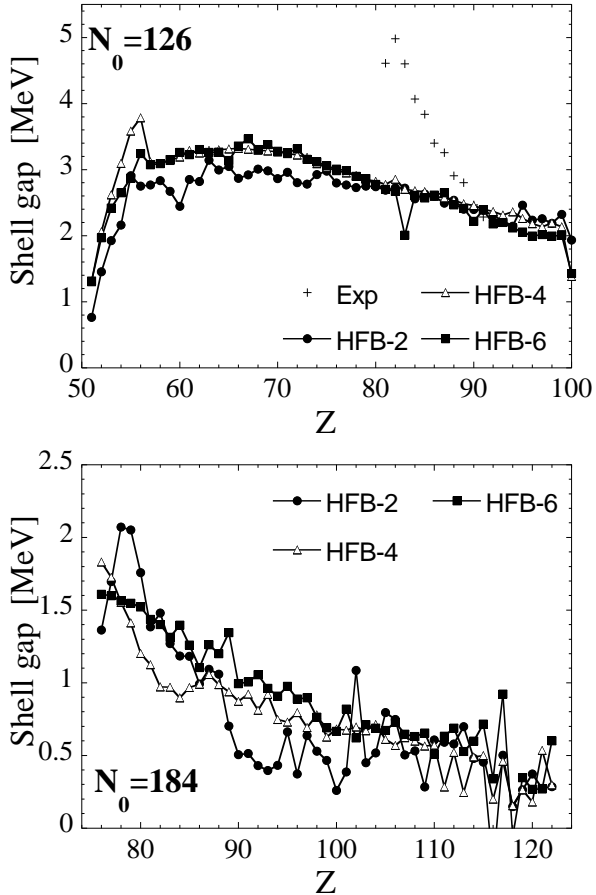


FIG. 9: $N_0 = 126$ (upper panel) and $N_0 = 184$ (lower panel) shell gap as a function of Z .

we have used an improved treatment of the center-of-mass correction [29], but although this makes a difference

to individual nuclei we have shown that the overall rms errors would have been essentially the same if we had used the same correction as in HFB-2 and HFB-3.

The extrapolations out to the neutron-drip line of all these different mass formulas are essentially equivalent. We thus see that the mass predictions required for the elucidation of the r-process are beginning to acquire a certain stability against changes in the underlying model. Nevertheless, it must be remembered that the acquisition of new mass data in the regions far from stability may well necessitate drastic changes to the underlying model.

Although the forces presented in this paper are equivalent from the standpoint of nuclear masses, there may still be significant differences as far as other quantities of astrophysical significance are concerned, e.g., fission properties, nuclear level densities, giant isovector dipole resonance (GDR), and beta-strength functions. Investigations along these lines has already begun, and it has been shown [48] that the measured positions of the GDR strongly favor the Skyrme forces BSk6 and BSk7 with their low effective mass of $M^* = 0.8M$; these calculations were made within the HFB plus Quasi-particle Random Phase Approximation (QRPA) framework (the second-RPA method being applied to estimate the higher QRPA effects). However, the interpretation of such calculations depends on the extra modelling, and the underlying approximations, of collective excitations through the QRPA method; further studies are needed.

Acknowledgements

M.S. and S.G. are FNRS Research Fellow and Associate, respectively. M.B. acknowledges support through a European Community Marie Curie fellowship. We wish to thank P.-H. Heenen for extensive discussions. This research was supported in part by the PAI-P5-07 of the Belgian Office for Scientific Policy and NSERC (Canada).

- [1] S. Goriely, F. Tondeur, and J. M. Pearson, At. Data Nucl. Data Tables **77** (2001) 311.
- [2] M. Samyn, S. Goriely, P.-H. Heenen, J.M. Pearson, and F. Tondeur, Nucl. Phys. **A700** (2002) 142.
- [3] S. Goriely, M. Samyn, P.-H. Heenen, J.M. Pearson, and F. Tondeur, Phys. Rev. C **66** (2002) 024326.
- [4] M. Samyn, S. Goriely, and J.M. Pearson, Nucl. Phys. **A725**, 69 (2003).
- [5] G. Audi and A. H. Wapstra, private communication (2001).
- [6] E. Garrido, P. Sarriguren, E. Moya de Guerra, P. Schuck, Phys. Rev. C **60** (1999) 064312.
- [7] F. Tondeur, S. Goriely, J.M. Pearson, and M. Onsi, Phys. Rev. C **62**, 024308 (2000).
- [8] M. Bender, P.-H. Heenen, and P.-G. Reinhard, Rev. Mod. Phys. **75**, 121 (2003).
- [9] G. E. Brown, J. H. Gunn, and P. Gould, Nucl. Phys. **46**, 598 (1963).
- [10] M. Barranco and J. Treiner, Nucl. Phys. **A351**, 269 (1981).
- [11] K. A. Brueckner and J. L. Gammel, Phys. Rev. **109**, 1023 (1958).
- [12] B. Friedman and V. R. Pandharipande, Nucl. Phys. **A361**, 502 (1981).
- [13] R. B. Wiringa, V. Fiks, and A. Fabrocini, Phys. Rev. C **38**, 1010 (1988).
- [14] W. Zuo, I. Bombaci, and U. Lombardo, Phys. Rev. C **60**, 024605 (1999).
- [15] W. Zuo, A. Lejeune, U. Lombardo, and J. F. Mathiot, Nucl. Phys. **A706**, 418 (2002).
- [16] A. N. James, P. T. Andrews, P. Kirkby, and B. G. Lowe, Nucl. Phys. **A138**, 145 (1969).
- [17] D. Vautherin and D. M. Brink, Phys. Rev. C **5**, 626 (1972).
- [18] J. P. Jeukenne, A. Lejeune, and C. Mahaux, Phys. Rep. **25**, 83 (1976).
- [19] C. Mahaux, P. F. Bortignon, R. A. Broglia, and C. H. Dasso, Phys. Rep. **120**, 1 (1985).
- [20] O. Bohigas, A. M. Lane, and J. Martorell, Phys. Rep. **51**, 267 (1979).

- [21] G. F. Bertsch and T. T. S. Kuo, Nucl. Phys. **A112**, 204 (1968).
- [22] V. Bernard and Nguyen Van Giai, Nucl. Phys. **A348**, 75 (1980).
- [23] M. Brack, J. Damgaard, A. S. Jensen, H. C. Pauli, V. M. Strutinsky, and C. Y. Wong, Rev. Mod. Phys. **44**, 320 (1972).
- [24] M. Farine, J. M. Pearson, and F. Tondeur, Nucl. Phys. **A696**, 396 (2001).
- [25] E. Chabanat, P. Bonche, P. Haensel, J. Meyer, R. Schaeffer, Nucl. Phys. **A635**, 231 (1998); Nucl. Phys. **A643**, 441(E) (1998).
- [26] M. Onsi and J. M. Pearson, Phys. Rev. C **65**, 047302 (2002).
- [27] P. Ring and P. Schuck, *The nuclear many-body problem*, Springer, New York (1980).
- [28] M. N. Butler, D. W. L. Sprung, and J. Martorell, Nucl. Phys. **A422**, 157 (1984).
- [29] M. Bender, K. Rutz, P.-G. Reinhard, and J. Maruhn, Eur. Phys. J. **A7**, 467 (2000).
- [30] P. Möller and J. R. Nix, At. Data Nucl. Data Tables **39**, 213 (1988).
- [31] P. Möller, J. R. Nix, W.D. Myers, and W.J. Swiatecki, At. Data Nucl. Data Tables **59**, 185 (1995).
- [32] G. Audi and A. H. Wapstra, Nucl. Phys. **A595**, 409 (1995).
- [33] D. Lunney, J. M. Pearson, and C. Thibault, Rev. Mod. Phys. **75**, 1021 (2003).
- [34] E. Nadjakov, K. Marinova and Yu. P. Gangrsky, At. Data and Nucl. Data Tables **56**, 133 (1994).
- [35] F. Buchinger, J. M. Pearson, and S. Goriely, Phys. Rev. C **64**, 067303 (2001).
- [36] Nguyen Van Giai and H. Sagawa, Phys. Lett. **B106**, 379 (1981).
- [37] M. Kutschera and W. Wójcik, Phys. Lett. **B325**, 271 (1994).
- [38] W. D. Myers and W. J. Swiatecki, Ann. Phys. **55**, 395 (1969).
- [39] J. M. Pearson and S. Goriely, Phys. Rev. C **64**, 027301 (2001).
- [40] D. H. Youngblood, Y.-W. Lui, and H. L. Clark, Phys. Rev. C **65**, 034302 (2002).
- [41] S.-O. Bäckman, A. D. Jackson, and J. Speth, Phys. Lett. **B56**, 209 (1975).
- [42] M. Bender, J. Dobaczewski, J. Engel, and W. Nazarewicz, Phys. Rev. C **65**, 054322 (2002).
- [43] J. Cugnon, P. Deneye, and A. Lejeune, Z. Phys. A **328**, 409 (1987).
- [44] R. B. Wiringa, V. Fiks, and A. Fabrocini, Phys. Rev. C **38**, 1010 (1988).
- [45] A. Akmal, V. R. Pandharipande, and D. G. Ravenhall, Phys. Rev. C **58**, 1804 (1998).
- [46] M. Sanchez-Vega, B. Fogelberg, H. Mach, R. B. E. Taylor, A. Lindroth, J. Blomqvist, A. Covello, and A. Gargano, Phys. Rev. C **60**, 024303 (1999).
- [47] K. A. Mezilev, Yu. N. Novikov, V. V. Popov, B. Fogelberg, and L. Spanier, Phys. Scripta. **T56**, 272 (1995).
- [48] S. Goriely, E. Khan, M. Samyn, Nucl. Phys. A, submitted